Composite beams with viscoelastic interaction. An application to laminated glass

Laura Galuppi

Gianni Royer-Carfagni

Department of Civil-Environmental Engineering and Architecture
University of Parma, Parco Area delle Scienze 181/A, I 43100 Parma, Italy
tel: +39-0521-905917, fax: +39-0521-905924, email: gianni.royer@unipr.it

Abstract

A practical way to calculate the response of laminated glass is to consider both glass and polymeric interlayer as linear elastic materials; the viscoelastic behavior of the polymer is evaluated assuming *equivalent* elastic moduli, that is, the relaxed moduli under constant strain after a time equal to the duration of the design action. Here, we analytically solve the time-dependent problem of simply-supported laminated-glass beams, modeling the response of the polymer by a Prony's series of Maxwell elements. The obtained results, in agreement with a full 3-D viscoelastic finite-element numerical analysis, emphasize that there is a noteworthy difference between the state of strain and stress calculated in the full-viscoelastic case or in the aforementioned "*equivalent*" elastic problem. The second approach gives in general results that are on the side of safeness, but the design may be too conservative for short-time actions, whose duration depends upon the polymer type.

1 Introduction

Three-layered sandwich structures that can be schematized as the composition of two external elastic elements bonded by one interlayer with anelastic response are commonly used

1

in modern constructions. The applications may range from structural insulating panels, consisting in a layer of polymeric foam sandwiched between two layers of structural board, to steel beams supporting concrete slabs connected by ductile studs, to wood elements made of layers glued together. Although the problem here considered is general and may apply to various cases, the particular application to which it will be specialized is that of laminated glass.

Laminated glass is a composite structure typically made of two glass plies bonded by a thermoplastic polymeric interlayer with a treatment in autoclave at high pressure and temperature. This process induces a strong chemical bond between materials, due to the union between hydroxyl groups along the polymer and silanol groups on the glass surface. In this way, safety in the the post-glass-breakage phase is increased because the fragments remain attached to the interlayer: risk of injuries is reduced and the damaged element maintains a certain cohesion that prevents catastrophic detachment from fixings.

In the pre-glass-breakage phase, the polymeric interlayers are too soft to present flexural stiffness *per se*, but they can provide shear stresses that constrain the relative sliding of the glass plies [4]. The degree of coupling of the two glass layers depends upon the shear stiffness of the polymeric interlayer [11]; thus, flexural stiffness is somehow intermediate between the two borderline cases usually referred to [16] as *layered limit*, i.e., frictionless relative sliding of the plies, and *monolithic limit*, i.e., perfect bonding of the plies. Since stress and strain in the monolithic limit are much lower than in the layered limit, appropriate consideration of the shear coupling offered by the interlayer is important to achieve an economical design. A number of studies have pursued this issue [3, 5, 12].

The response of the polymer is highly viscoelastic and temperature dependent. There are three main commercial polymeric films: Polyvinyl Butyral (PVB), Ethylene Vinyl Acetate (EVA), and Ionoplastic polymers (IP) [5, 6]. PVB is a polyvinyl acetate with addition of softeners that imparts plasticity and toughness, enhancing adhesion-strength and increasing glass transition temperature T_g up to $20 - 25°C$. Commercial EVA is a polyolefine with addiction of vinyl acetate that improves strength and ultimate elongation, to attain mechanical properties that are similar to PVB. A somehow innovative materials is IP, a ionoplast polymer that, when compared with PVB, presents higher stiffness ($> 100×$PVB), strength ($> 5×$PVB), glass-transition temperature ($T_g \sim 55°C$).

In general, the rheological properties are furnished by the manufacturer in the form of tables, which record the relaxed shear modulus of the polymer under constant shear strain as a function of temperature and time. Such values are used in the common design practice, by considering the polymer as a linear elastic materials whose shear modulus is chosen according to the environmental temperature and the characteristic duration of the design load [7]. Depending upon polymer type, room-temperature T and characteristic load-duration t_0, the relaxed shear modulus of the interlayer may vary from 0.01 MPa (PVB at $T = +60°C$ under permanent load) up to 300 MPa (IP at $T = 0°C$ and $t_0 = 1$ sec). Assumption that both glass and polymer are linear elastic allows for drastic simplifications in

the structural analysis and simplified approaches may also be provided for ready calculations in the cases of most practical interest. For example, the well-known model by Newmark [15] considers the interaction of two beams bonded by shear connectors that provide a linear and continuous relationship between the relative interface slip and the corresponding shear stress, and may be conveniently used when the bending moment is known *a priori*, as in the case of statically-determined structures. A comprehensive discussion about various possible simplified methods of analysis can be found in [10].

A more precise rheological analysis should consider the polymer as a linear viscoelastic materials, that can be usually interpreted by a Prony's series of units arranged in the Maxwell-Wiechert model [19]. The parameters that define the constitute properties may be found through creep or relaxation tests [14, 17], or by measuring the response to cyclic oscillations [2, 13]; in some cases they are directly furnished by the manufactures [7]. Temperature dependence may be taken into account using the Williams-Landel-Ferry model [20]. However, a full viscoelastic analysis is seldom performed in the design practice, because it is time consuming and requires a special software. Numerical experiments can be found in the technical literature on specific particular examples, comparing the results with those obtained through the aforementioned linear solution that makes use of the relaxed modulus for the polymer. However, to our knowledge, no systematic study exists that discusses the viscoelastic interaction of the glass plies and, in particular, the specific effects of various different relaxation times characterizing the Maxwell-Wiechert model.

Here, we analytically solve the time-dependent problem of a laminated-glass simply-supported beam under constant loading, modeling the response of the polymer by a Prony's series in the Maxwell-Wierchert model. It will be shown that the "memory effect" of viscoelasticity may affect the gross response of the laminated glass beams, producing in same cases a noteworthy differences with respect to those practical approaches that consider the secant stiffness of the polymer only. The influence of the various parameters of the Prony's series, and in particular the effects of the various relaxation times, is discussed. Applicative examples to the most commercial types of polymers used as interlayers are developed.

2   Composite sandwich beam with viscoelastic interaction

Consider the simply-supported sandwich beam of length L shown in figure 1, composed of two external linear elastic plies of thickness h_1 and h_2, bonded by a thin viscoleastic interlayer of thickness h. The structures is loaded under a generic load per unit length $p(x,t)$, not necessarily time-independent and uniformly distributed.

This example perfectly adapts to the case of laminated glass, where the external plies are made of glass, whereas the interlayer is a polymeric sheet. In the following, without loosing generality, we will refer to this particular application. Therefore, the two external glass layers present linear-elastic response, with Young's modulus E, whereas the interlayer is
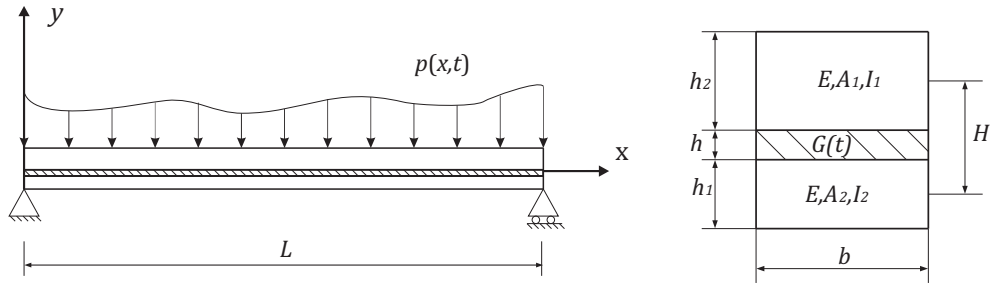
Figure 1: Sandwich beam composed of two linear-elastic external layers, bonded by a viscoelastic interlayer.

made of a viscoelastic polymer, with time-dependent shear modulus $G(t)$.

2.1   Viscoelastic constitutive response

The most general model for linear viscoelasticity is the well-known *Maxwell-Wiechert model* [19], schematically represented in Figure 2, which combines in parallel a series of Maxwell spring-dashpot units (with spring constant G_i and dashpot viscosity η_i) and a Hookean spring. This model takes into account that relaxation does not occur at a single time-scale, but at a number of different time scales, each one associated with a Maxwell unit.
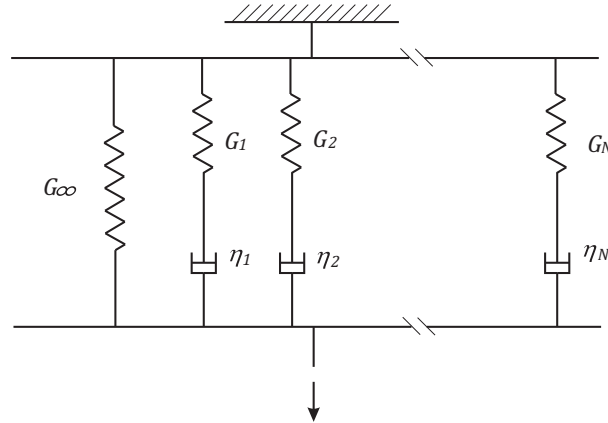

Figure 2: Schematic representation of the Maxwell-Wiechert model.

When subjected to a fixed constant shear-strain, the shear modulus of the viscoelastic material decays with time according to an expression usually referred to as Prony series, defined as

$$G(t) = G_\infty + \sum_{i=1}^{N} G_i e^{-t/\tau_i} = G_0 - \sum_{i=1}^{N} G_i(1 - e^{-t/\tau_i}), \qquad (2.1)$$

where G_∞ represents the long-term shear modulus (when the material is totally relaxed), whereas the terms G_i and $\tau_i = \frac{\eta_i}{G_i}$, $i = 1..N$ are respectively the relaxation shear moduli and the relaxation times, associated with the $i - th$ Maxwell element composing the Maxwell-Wiechert unit (Figure 2). The instantaneous shear modulus G_0 is thus given by $G_\infty + \sum_{i=1}^{N} G_i$. Whenever $N = 1$, the Maxwell-Wiechert model reduces to the *Standard Linear Solid Model*, that combines a Maxwell spring-dashpot element and a Hookean spring in parallel.

When the shear strain varies with time, i.e. $\gamma = \gamma(t)$, under the hypothesis of linear viscoelasticity, the corresponding shear stress $\tau(x,t)$ can be obtained by the Boltzmann superposition principle [8], that can be equivalently written in the forms

$$\tau(t) = G(t)\gamma(0) + \int_0^t G(t - \xi)\frac{\partial \gamma(\xi)}{\partial \xi}d\xi = G(0)\gamma(t) - \int_0^t \frac{\partial G(t - \xi)}{\partial \xi}\gamma(\xi)d\xi \,. \qquad (2.2)$$

Clearly, when the imposed shear strain is constant in time ($\gamma = $ const), equation (2.2) reduces to $\tau(t) = G(t)\gamma$. Whenever the strain is time-dependent, the stress depends on both the current strain and the strain history up to the current time, through the hereditary integral appearing in (2.2). This implies, for example, that when the applied strain increases with time, the relaxation of the correspondent stress is delayed with respect to the relaxation of the shear modulus calculated according to (2.1) because, roughly speaking, strain increases *before* stress has the time to relax.

The aforementioned observation is a keypoint for the present work. In fact, the common design practice for laminated glass consists in modeling the polymer as a linear elastic material, taking at each instant t its equivalent elastic modulus to be $G(t)$ calculated according to the expression (2.1). In other words, for a load history leading to the shear strain $\gamma(t)$, the shear stress $\tau_{inst}(t)$ is assumed not to be given by (2.2) but of the form

$$\tau_{inst}(t) = G(t)\gamma(t) \,. \qquad (2.3)$$

However, if the strain history is sufficiently fast, at each instant t the modulus G does not have the time to reach the value $G(t)$ given by (2.1). Figure 3 shows the qualitative comparison between the shear stress evaluated through equation (2.2) (continuous line) and through the *approximation* (2.3) (dashed line) in the case of a linear increasing strain $\gamma(t) = \alpha t$, for the case of a material modeled through a Prony's series with $N = 1$ and relaxation time τ_1.
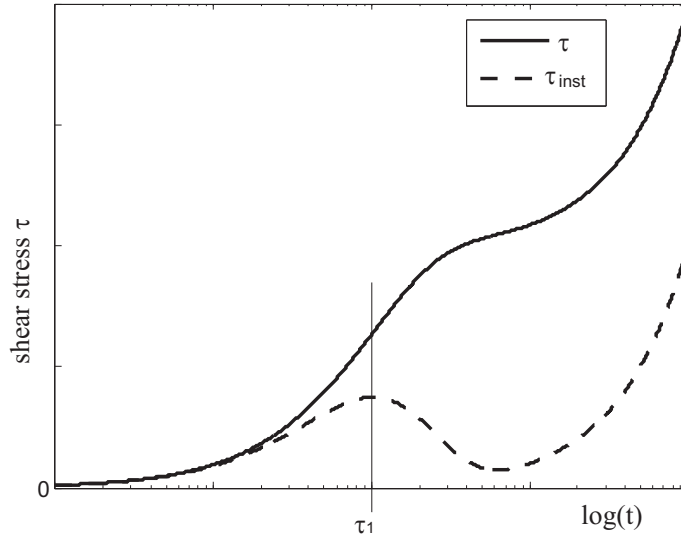
Figure 3: Qualitative comparison between the shear stress τ, evaluated through equation (2.2), and τ_{inst}, evaluated through (2.3), in the case of linear-increasing shear strain.

It is evident the aforementioned "delay" in the stress response and the consequently stress stiffening. It will be demonstrated later on the relevance of such a delay in the global response of a laminated glass beam.

2.2 Governing integral-differential equations

The analysis of a linear-elastic sandwich beam of the type represented in Figure 1 has already been presented elsewhere. Referring to [10] for the details, here the governing equations are briefly recalled and specialized to the case of viscoelasticity.

With reference to Figure 1, a right-handed orthogonal reference frame (x, y) is introduced with x parallel to the beam axis, supposed horizontal, and y directed upwards. The glass-polymer bond is supposed to be perfect and the interlayer normal strain in direction y is negligible. Under the hypothesis that strains are small and the rotations moderate, the kinematics is completely described by the vertical displacement $v(x, t)$, the same for the three layers, and the horizontal displacements $u_1(x, t)$ and $u_2(x, t)$ of the centroid of the upper and lower layers, respectively. The transversal displacement $v(x, t)$ is positive if in the same direction of increasing y, the transversal load $p(x, t) > 0$ if directed downwards, while the bending moment $M(x, t)$ is such that $M(x, t) > 0$ when $v''(x, t) > 0$. In the sequel, $(')$ will denote differentiation with respect to the variable x, whereas $(\cdot)$ will represent differentiation with respect to t.

Let us define

$$A_i = h_i b, \ I_i = \frac{bh_i^3}{12} \ (i = 1, 2), \ H = t + \frac{h_1 + h_2}{2}, \ A^* = \frac{A_1 A_2}{A_1 + A_2}, \ I_{tot} = I_1 + I_2 + A^* H^2, \quad (2.4)$$

and observe that I_{tot} represents the moment of inertia of the full composite section, corresponding to the *monolithic* limit.

It can be verified [10] that the shear strain in the interlayer is constant through its thickness h and given by

$$\gamma(x, t) = \frac{1}{h} [u_1(x, t) - u_2(x, t) + v'(x, t)H]. \quad (2.5)$$

From (2.2), the sher stress in the interlayer can be written as

$$\tau(x, t) = G(0)\gamma(x, t) - \int_0^t \frac{\partial G(t - \xi)}{\partial \xi} \gamma(x, \xi) d\xi, \quad (2.6)$$

so that the equilibrium in the y direction results to be [10]

$$E(I_1 + I_2)v''''(x, t) - b\left\{ G(0)\gamma'(x, t) - \int_0^t \frac{\partial G(t - \xi)}{\partial \xi} \gamma'(x, \xi) d\xi \right\} H + p(x, t) = 0. \quad (2.7)$$

This expression can be easily justified because the quantity $\left\{ G(0)\gamma'(x, t) - \int_0^t \frac{\partial G(t - \xi)}{\partial \xi} \gamma'(x, \xi) d\xi \right\}$ coincides with $\tau'(x, t)$, i.e., the derivative of the the shear stress in the interlayer. Figure 4.a shows the the equilibrium of an infinitesimal beam voussoir, divided into two pieces by an ideal horizontal cut in the interlayer at the level s^* (s^* may be chosen arbitrarily). It is then clear that the shear stress $\tau(x, t)$ gives a distributed torque per unit length equal to $-b\tau(h_1/2 + s^*)$ in the upper piece, and $-b\tau(h_2/2 + s - s^*)$ in the lower piece. Consequently, condition (2.7) represents the equilibrium in the $y-$direction under bending of the whole composite package, i.e., $EIv''''(x, t) + m'(x, t) + p(x, t) = 0$, with $I = I_1 + I_2$ and

$$m(x, t) = -b\tau(x, t)(h_1/2 + s^*) - b\tau(x, t)(h_2/2 + s - s^*) = -b\tau(x, t)H. \quad (2.8)$$

It is the effect of such a distributed torque due the shear stress transferred by the interlayer, that increases the stiffness of the laminated glass beam.
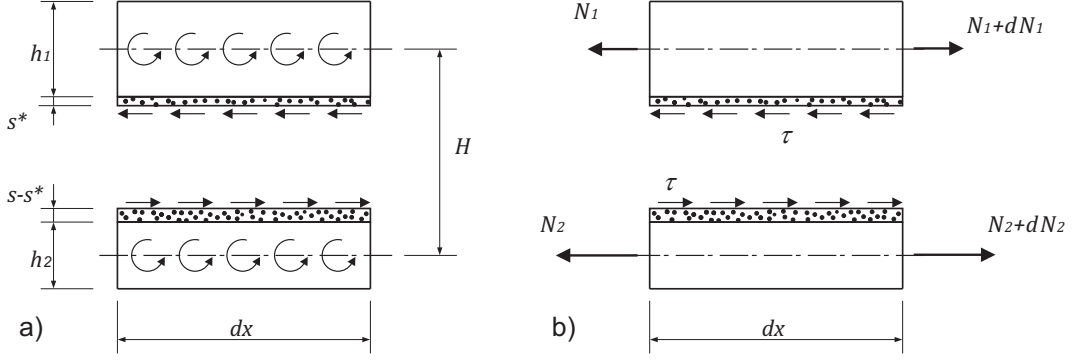
Figure 4: Equilibrium of an infinitesimal voussoir of the composite package.

Furthermore, equilibrium in x direction of each one of the two pieces (Figure 4.b) leads to

$$EA_1 u_1''(x,t) = b\left\{ G(0)\gamma(x,t) - \int_0^t \frac{\partial G(t-\xi)}{\partial \xi}\gamma(x,\xi)d\xi \right\},$$ (2.9)

$$EA_2 u_2''(x,t) = -b\left\{ G(0)\gamma(x,t) - \int_0^t \frac{\partial G(t-\xi)}{\partial \xi}\gamma(x,\xi)d\xi \right\}.$$ (2.10)

In fact, the axial force in the $i - th$ glass layer is $N_i = EA_i u_i'(x,t)$, so that (2.9) and (2.10) represent the axial equilibrium of the two glass plies under the mutual shear force per unit length $b\tau(x,t)$ transmitted by the polymeric interlayer, i.e., $EA_1 u_1''(x,t) = -EA_2 u_2''(x,t) = b\tau(x,t)$.

The boundary conditions may be of two classes: essential (geometric) and natural (force). For this case, at the boundary $\bar{x} = 0$ or $\bar{x} = L$, $\forall t$ one can prescribe [10]:

$$
\begin{aligned}
&E(I_1 + I_2)v'''(\bar{x},t) + b\left(G(0)\gamma(\bar{x},t) - \int_0^t \frac{\partial G(t-\xi)}{\partial \xi}\gamma(\bar{x},\xi)d\xi \right) = 0 \;\; \text{or} \;\; v(\bar{x},t) = 0\,, \\
&E(I_1 + I_2)v''(\bar{x},t) = 0 \;\; \text{or} \;\; v'(\bar{x},t) = 0\,, \\
&EA_1 u_1'(\bar{x},t) = 0 \;\; \text{or} \;\; u_1(\bar{x},t) = 0\,, \\
&EA_2 u_2'(\bar{x},t) = 0 \;\; \text{or} \;\; u_2(\bar{x},t) = 0\,,
\end{aligned}
$$ (2.11)

In the case of a simply supported beam, first and second of (2.11) are respectively satisfied by the essential conditions $v(\bar{x},t) = 0$ and the natural conditions $v''(\bar{x},t) = 0$ at $\bar{x} = 0$ and $\bar{x} = L$. For what concerns the last two of (2.11), observe that

- if the beam is axially constrained at one of its ends, the conditions are identically satisfied if $u_1(\bar{x},t) = u_2(\bar{x},t) = 0$ at the considered edge $\bar{x} = 0$ or $\bar{x} = L$;

- if the beam is not axially constrained and the borders are traction-free, then $EA_i u_i'(\bar{x}, t) = N_i(\bar{x}, t) = 0$, $i = 1, 2$ at the considered edge $\bar{x} = 0$ or $\bar{x} = L$.

As it is shown in the sequel, equations (2.7), (2.9) and (2.10) can be re-arranged in one partial integro-differential equation for the function $v(x, t)$ with the same procedure outlined in [10]. To illustrate, observe that equations (2.9) and (2.10) provide condition

$$A_1 u_1''(x, t) = -A_2 u_2''(x, t), \qquad (2.12)$$

from which, up to a Rigid Body displacement,(see [10]),

$$u_2(x, t) = -\frac{A_1}{A_2} u_1(x, t), \qquad (2.13)$$

which implies that $N_1(x, t) = -N_2(x, t)$. Observe now that the bending moment in the ith glass layer, $i = 1, 2$, is $M_i(x, t) = EI_i v''(x, t)$. Consequently, the resulting bending moment in the whole cross-section of the composite beam (see Figure 4) is $M(x, t) = M_1(x, t) + M_2(x, t) + N_2(x, t)H = M_1(x, t) + M_2(x, t) - N_1(x, t)H$, that is

$$M(x, t) = E(I_1 + I_2)v''(x, t) + EA u_2'(x, t)H = E(I_1 + I_2)v''(x, t) - EA u_1'(x, t)H. \qquad (2.14)$$

From this, one finds the relationships

$$\begin{cases} HA_1 u_1'(x, t) = (I_1 + I_2)v''(x, t) - M(x, t)/E, \\[2mm] HA_2 u_2'(x, t) = -(I_1 + I_2)v''(x, t) + M(x, t)/E. \end{cases} \qquad (2.15)$$

By substituting (2.15) in (2.5) and, afterwards, in (2.7), one finds the governing partial integral-differential equation for the function $v(x, t)$ in the form

$$E(I_1 + I_2)v''''(x, t) - \frac{bI_{tot}}{hA^*}\left\{ G(0)v''(x, t) - \int_0^t \frac{\partial G(t - \xi)}{\partial \xi} v''(x, \xi)d\xi \right\} +$$

$$+ \frac{b}{hEA^*}\left\{ G(0)M(x, t) - \int_0^t \frac{\partial G(t - \xi)}{\partial \xi} M(x, \xi)d\xi \right\} + p(x, t) = 0. \qquad (2.16)$$

This form is more convenient whenever the beam is statically determined, i.e., when the bending moment $M(x, t)$ is defined by the external loads. Equation (2.16) can be considered as the viscoelastic generalization of Newmark's equation [15].

In the particular case of time-independent load, $p(x,t) = \widetilde{p}(x)$, the equilibrium equation (2.16) reduces to

$$
E(I_1 + I_2)v''''(x,t) - \frac{bI_{tot}}{hA^*}\left\{G(0)v''(x,t) - \int_0^t \frac{\partial G(t-\xi)}{\partial \xi}v''(x,\xi)d\xi\right\}+
$$
$$
+ \frac{b}{hEA^*}G(t)\widetilde{M}(x) + \widetilde{p}(x) = 0 \,, \quad (2.17)
$$

in which $\widetilde{M}(x)$ is the bending moment due to $\widetilde{p}(x)$. In this expression the second and the third terms represent the effect of the bonding offered by the polymeric interlayer. In particular, the second term represents the interfacial shear strain, dependent on the shear strain history; the effect of such a contribution on the behavior of the sandwich structure is, in general, benefic.

A general method to solve (2.16) is to make use of Laplace transforms $\mathfrak{L}(\cdot)$ and the anti-transform $\mathfrak{L}^{-1}(\cdot)$, using the fact that the convolution integrals can be written as

$$
\begin{cases}
G(0)v''(x,t) - \int_0^t \frac{\partial G(t-\xi)}{\partial \xi}v''(x,\xi)d\xi = \mathfrak{L}^{-1}\left\{s\mathfrak{L}(G(t))\mathfrak{L}(v''(x,t))\right\}, \\[2mm]
G(0)M(x,t) - \int_0^t \frac{\partial G(t-\xi)}{\partial \xi}M(x,\xi)d\xi = \mathfrak{L}^{-1}\left\{s\mathfrak{L}(G(t))\mathfrak{L}(M(x,t))\right\}.
\end{cases}
\quad (2.18)
$$

However, for the case of constant loading and when the Prony's series contains several terms, it is more convenient to perform an analysis *à la* Galerkin.

2.3 Solution *via* Galerkin Analysis

A method for solving equation (2.16) is to apply the Galerkin's method [9] for the spatial domain, i.e. to express the vertical displacement $v(x,t)$ by a series expansion of the form

$$
v(x,t) = \sum_{j=1}^{M} a_j(t)\phi_j(x) \qquad (2.19)
$$

where $\phi_j(x)$ is the j-th shape function and $a_j(t)$ is the corresponding time-dependent amplitude. The spatial shape functions have to satisfy the boundary condition and to be linear independent; if the $\phi_j(x)$ are choose to be orthogonal one to another, i.e.,

$$\int_0^L \phi_j(x)\phi_k(x)dx = \begin{cases} K & if\ j = k\,, \\ 0 & if\ j \neq k\,, \end{cases} \qquad (2.20)$$

(where K is a generic constant) the resulting set of equations will be uncoupled. An appropriate choice of the shape functions for the case of simply supported beams is

$$\phi_j(x) = \sin\frac{\pi x j}{L}\,. \qquad (2.21)$$

Consequently, $a_j(t)$ gives the time-dependent maximum sag of the beam $v_{max}(t) = v(L/2, t) = |a_j(t)|$, associated with the j-th shape function.

By defining $\lambda_j = \frac{\phi_j''''(x)}{\phi_j(x)} = \frac{j^4\pi^4}{L^4}$ and $\mu_j = \frac{\phi_j''(x)}{\phi_j(x)} = -\frac{j^2\pi^2}{L^2}$, the expansion (2.19) for $v(x,t)$ is substituted into the equilibrium equation (2.16). The result is

$$E(I_1 + I_2)\sum_{i=1}^{M} a_i(t)\lambda_i\phi_i(x) - \frac{bI_{tot}}{hA^*}\sum_{i=1}^{M}\mu_i\phi_i(x)\Big\{G(0)a_i(t) - \int_0^t \frac{\partial G(t-\xi)}{\partial \xi}a_i(\xi)d\xi\Big\} +$$

$$+ \frac{b}{hEA^*}\Big\{G(0)M(x,t) - \int_0^t \frac{\partial G(t-\xi)}{\partial \xi}M(x,\xi)d\xi\Big\} + p(x,t) = 0\,. \quad (2.22)$$

Multiplying each term for the $j - th$ shape function, integrating over the spatial domain and applying (2.20), where $K = \frac{L}{2}$, one finally obtains

$$E(I_1 + I_2)\frac{L}{2}a_j(t)\lambda_j - \frac{bI_{tot}}{hA^*}\frac{L}{2}\mu_j\Big\{G(0)a_j(t) - \int_0^t \frac{\partial G(t-\xi)}{\partial \xi}a_j(\xi)d\xi\Big\} +$$

$$+ \frac{b}{hEA^*}\Big\{G(0)\int_0^L M(x,t)\phi_j(x)dx - \int_0^t \frac{\partial G(t-\xi)}{\partial \xi}\Big[\int_0^L M(x,\xi)\phi_j(x)dx\Big]d\xi\Big\} +$$

$$+ \int_0^L p(x,t)\phi_j(x)dx = 0\,, \quad (2.23)$$

In the case of constant loading, (2.23) reduces to

$$E(I_1 + I_2)j\frac{j^4\pi^4}{L^4}a_j(t) + \frac{bI_{tot}}{hA^*}j\frac{j^2\pi^2}{L^2}\Big\{G(0)a_j(t) - \int_0^t \frac{\partial G(t-\xi)}{\partial \xi}a_j(\xi)d\xi\Big\} +$$

$$+ \frac{b\,G(t)}{hEA^*}\int_0^L \widetilde{M}(x)\sin\frac{\pi x j}{L}dx + \int_0^L \widetilde{p}(x)\sin\frac{\pi x j}{L}dx = 0\,. \quad (2.24)$$

But the load function $\widetilde{p}(x)$ can also be expanded into a Fourier sine of the form

$$\widetilde{p}(x) = \sum_{n=1}^{\infty} c_n \sin \frac{n\pi x}{L} \; , \qquad c_n = \frac{1}{L} \int_0^L \widetilde{p}(x) \sin \frac{n\pi x}{L} dx \; . \tag{2.25}$$

Observing that in a simply supported beam the corresponding bending moment is given by $\widetilde{M}(x) = \sum_{n=1}^{\infty} \frac{L^2}{n^2\pi^2} c_n sin \frac{n\pi x}{L}$, such a procedure allows to obtain, from (2.24), the set of uncoupled equations for the time-dependent amplitude $a_j(t)$

$$E(I_1+I_2)\frac{j^4\pi^4}{L^4} a_j(t) + \frac{bI_{tot}}{hA^*}\frac{j^2\pi^2}{L^2}\Big\{ G(0)a_j(t) - \int_0^t \frac{\partial G(t-\xi)}{\partial \xi} a_j(\xi)d\xi \Big\} + \frac{bG(t)}{hEA^*}\frac{L^2}{j^2\pi^2}c_j + c_j = 0 \; . \tag{2.26}$$

In the sequel, the paradigmatic case of a simply-supported beam subjected to a sinusoidal load will be discussed.

3 Case study: simply supported laminated glass beam under sinusoidal loading

Suppose that the simply-supported laminated glass beam is subjected to a time-independent sinusoidal loading $\widetilde{p}(x)$ to which corresponds the bending moment $\widetilde{M}(x)$ given by

$$\widetilde{p}(x) = p_0 \sin \frac{\pi x}{L} \; , \quad \widetilde{M}(x) = \frac{L^2}{\pi^2} p_0 \sin \frac{\pi x}{L} \; . \tag{3.27}$$

3.1 Full viscoelastic solution

Equation (2.17) reduces to

$$E(I_1+I_2)v''''(x,t) + \frac{bI_{tot}}{hA^*}\Big\{ G(0)a_1(t) - \int_0^t \frac{\partial G(t-\xi)}{\partial \xi} v''(x,\xi)d\xi \Big\} + \frac{bG(t)}{hEA^*}\frac{L^2}{\pi^2} p_0 + p_0 = 0 \; , \tag{3.28}$$

Hence, the exact solution for the vertical displacement (2.19) is given by

$$v(x,t) = a_1(t) \sin \frac{\pi x}{L} \; , \tag{3.29}$$

where the time-dependent amplitude $a_1(t)$ is the solution of the integral-differential equation

$$E(I_1 + I_2)a_1(t)\frac{\pi^4}{L^4} + \frac{bI_{tot}}{hA^*}\frac{\pi^2}{L^2}\left\{G(0)a_1(t) - \int_0^t \frac{\partial G(t-\xi)}{\partial \xi}a_1(\xi)d\xi\right\} + \frac{b\,G(t)}{hEA^*}\frac{L^2}{\pi^2}p_0 + p_0 = 0\,.$$
$$\tag{3.30}$$

Obviously, $a_1(t)$ represents the maximum sag of the beam at the instant t.

By substituting for $G(t)$ the expression (2.1), the integral differential equation (3.30) for the time-dependent amplitude $a_1(t)$ may be rearranged in the form

$$a_1(t) + \int_0^t \sum_{i=1}^N A_i e^{-\frac{(t-\xi)}{\tau_i}}a_1(\xi)d\xi = f(t)\,,\tag{3.31}$$

where

$$A_i = \frac{bI_{tot}\pi^2 G_i}{hA^*L^2\tau_i}\frac{1}{\frac{E(I_1+I_2)\pi^4}{L^4} + \frac{bI_{tot}\pi^2 G_0}{hA^*L^2}}\,,\tag{3.32}$$

$$f(t) = -p_0\left[\frac{b\left(G_\infty + \sum_{i=1}^N G_i e^{-t/\tau_i}\right)L^2}{hA^*E\pi^2} + 1\right]\frac{1}{\frac{E(I_1+I_2)\pi^4}{L^4} + \frac{bI_{tot}\pi^2 G_0}{hA^*L^2}}\,.\tag{3.33}$$

Whenever $N = 1$, i.e., the polymer response can be modeled thorough a Standard Linear Solid Model, equation (3.31) may be easily solved by using the Laplace transform, obtaining

$$a_1(t) = f(t) - A_1\int_0^t e^{-\frac{(t-\xi)}{\tau_1}}f(\xi)d\xi\,.\tag{3.34}$$

In the most general case, the solution of equation (3.31) can be represented in the form [18]

$$a_1(t) = f(t) + \int_0^t \sum_{i=1}^N B_i e^{\mu_i(t-\xi)}f(\xi)d\xi\,,\tag{3.35}$$

where the unknown constants μ_i are the root of the algebraic equation:

$$\sum_{i=1}^{N} \frac{A_i}{z + 1/\tau_i} + 1 = 0 \,, \tag{3.36}$$

and the coefficient B_i can be found from the linear system of algebraic equations

$$\sum_{i=1}^{N} \frac{B_i}{-1/\tau_m - \mu_i} + 1 = 0 \qquad m = 1, ..., n \,. \tag{3.37}$$

In the sequel, this analysis will be referred to as the *Full Viscoelastic* Solution (FVS).

3.2   The "secant stiffness" solution

As already mentioned in Section 2.1, the common design practice of laminated glass is to neglect the delayed response consequent to Boltzmann superposition formula (2.2), and assume that the shear stress in the interlayer is simply of the form $\tau_S(t) = G(t)\gamma(t)$, where $\gamma(t)$ is the strain in the polymer, whereas $G(t)$ is given by (2.1). This is equivalent to assume that at each instant t the stiffness of the polymer is the same that it would exhibit if the strain had been kept constant for the whole load history. In other words, the shear modulus used in the calculations is that corresponding to the secant stiffness at the end of a constant-strain process; because of this, the solution obtained under this simplifying assumption will be referred to as the *Secant Stiffness Solution* (SSS). Parameters associated with it will be indicated with the suffix S.

In the SSS, the governing equation (2.16) simplifies in the form

$$E(I_1 + I_2)v_S''''(x,t) + \frac{bI_{tot}}{hA^*}G(t)v_S''(x,t) + \frac{bG(t)}{hEA^*}M(x,t) + p(x,t) = 0 \,. \tag{3.38}$$

When the load is sinusoidal and time-independent as *per* (3.27), one has $v_S(x,t) = a_S(t)\sin\frac{\pi x}{L}$, where $a_S(t)$ solves

$$E(I_1 + I_2)a_S(t)\frac{\pi^4}{L^4} + \frac{bI_{tot}}{hA^*}\frac{\pi^2}{L^2}G(t)a_S(t) + \frac{bG(t)}{hEA^*}\frac{L^2}{\pi^2}p_0 + p_0 = 0 \,. \tag{3.39}$$

This is an algebraic equation that can be readily solved since $G(t)$ is known.

4 Comparison between the "full viscoelastic" and the "secant stiffness" solutions

Results obtainable with the full viscoelastic approach are now compared with those obtainable through the secant stiffness approach (3.39) and with the numerical solutions of a FEM model, accounting for time-dependent material behavior of the interlayer in the composite package. Numerical simulations have been made with the FEM code Abaqus, using a 3-D mesh with solid 20-node quadratic bricks with reduced integration, available in the program library [1]. The structured mesh has been created by dividing the length of the beam into 50 elements, its width into 10 elements and the thickness of each glass ply into 3 elements.

As a representative example, consider the case of a laminated-glass beam under the sinusoidal load (3.27), with $p_0 = 0.75$ N/m. With the notation of Figure 1, assumed parameters are $L = 3000$ mm, $b = 500$ mm, $h_1 = h_2 = 10$ mm, $s = 0.76$ mm, $E = 70000$ MPa, while the interlayer shear modulus $G(t)$ is given by (2.1).

4.1 Influence of the polymer shear modulus. Static analyis

First of all, it is useful to point out the influence of the interlayer-stiffness itself on the response of the laminated glass beam, by considering both material (glass and polymer) to be linear elastic and time-independent. Such static analysis has been discussed at length in [10] and here we recall the main results.

The response of laminated glass beams may vary between two borderline cases [16]: i) the *layered limit*, corresponding to $G \rightarrow 0$ so that the beam is composed of free-sliding glass plies, ; ii) the *monolithic limit*, with $G \rightarrow \infty$, where no relative slippage between the glass plies occurs. The flexural response turns out to be that of a beam whose cross section has moment of inertia I that, recalling the definitions (2.4), takes the value $I = I_1 + I_2$ for the layered limit and $I = I_{tot}$ in the monolithic limit. In general, the actual response is intermediate, depending upon the shear stiffness of the polymeric interlayer, through its shear modulus G.

Figure 5 shows the values of the maximum sag as a function of G, when this is varied from 10^{-4} MPa to 10^2 MPa. It is evident form the graph that for values of G higher than, approximatively, 10 MPa, the laminated glass beam exhibits a monolithic behavior, whereas for $G < 10^{-3}$ MPa the layered limit is attained. Of course, such threshold values depend on the geometric and mechanical properties of the beam, as well as on the boundary and loading conditions. However, for the most recurrent cases in the design practice for laminated glass, they may be considered reference values.
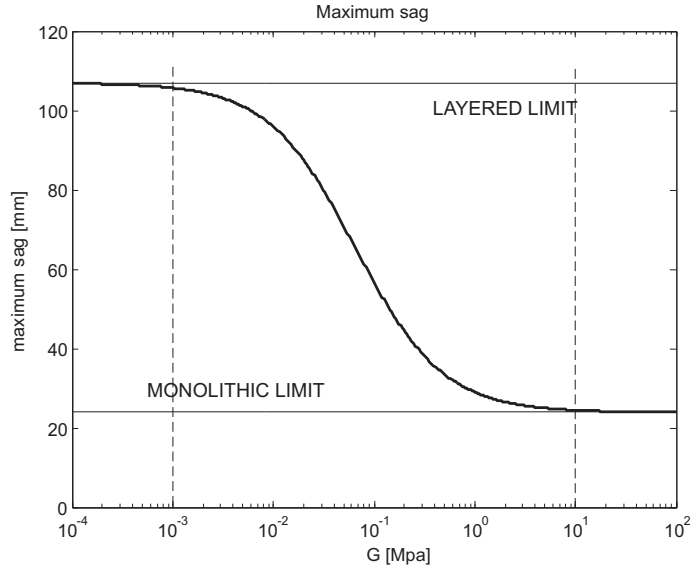
Figure 5: Simply supported beam under a sinusoidal load: maximum sag for different values of the shear modulus G of the interlayer (static analysis).

4.2   Influence of viscosity. Discussion

Two different viscoelastic material are here taken into account, for the sake of comparison. The first one, referred to as *Material A* can be model thorough a Standard Linear Solid Model, where in (2.1) $N = 1$ and $G_0 = 471$ MPa, $G_1 = 0.999G_0$, $\tau_1 = 1$ s. The full viscoelastic solution $a_1(t)$ may evaluated through equation (3.34). The correspondent maximum sag $v_{max} = |a_1(t)|$ is plotted as a function of time in Figure 6, where the graph is compared with the Secant Stiffness Solution as well as with numerical experiments.

It is important to note that the maximum sag of the laminated beam assumes values comprised between:

- the "instantaneous solution" v_{max0}, i.e., the solution associated with $G(t) = G_0$; such a limit is attained for $t < \tau_1$;

- the "long-term solution" $v_{max\infty}$, associated with $G(t) = G_\infty$.

Observed that the deformation of the FVS is time-increasing and, as already pointed out in Section 2.1, there is a delay in the material stress response with respect to the SSS. Consequently, the response of the laminated glass beam is stiffer than the response evaluated through the Secant Stiffness approach, and the beneficial effect of the shear stress transferred among the glass plies by the interlayer is higher. It is also evident that numerical experiments are in complete agreement with the FVS.
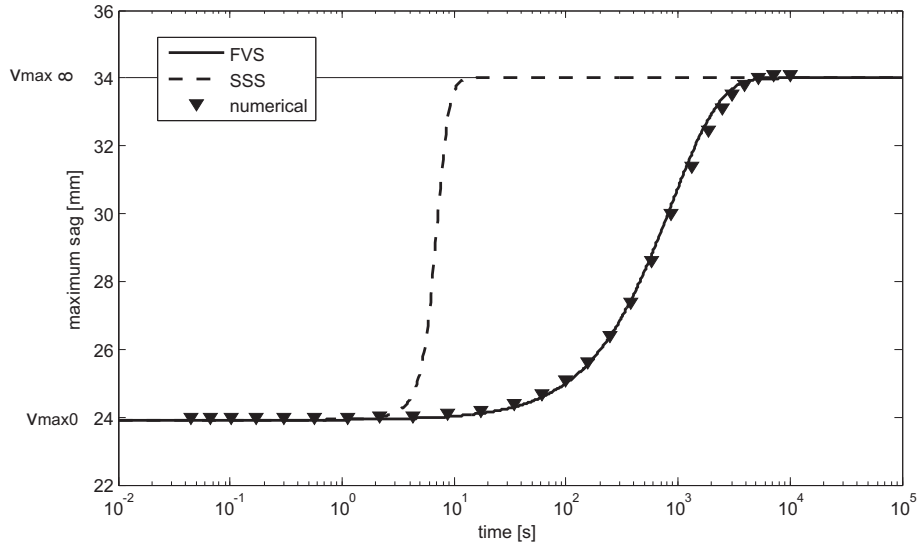
Figure 6: *Material A*: comparison of the maximum sag obtained with: the Full Viscoelastic Solution (FVS), the Secant Stiffness Solution (SSS), numerical experiments.

Consider then the second case for *Material B*, whose instantaneous shear modulus is $G_0 = 471$ MPa and exhibits three different relaxations (three terms in the Prony's series), at times $\tau_1 = 10^{-2}$ s, $\tau_2 = 1$ s and $\tau_3 = 10^2$ s with corresponding moduli $G_1 = 0.99G_0$, $G_2 = 0.009G_0$ and $G_3 = 0.0009G_0$. Figure 7 shows again the comparison between the maximum sag obtained by the FVS of (3.35) and the SSS of (3.39). The numerical experiments confirm again the exactness of the FVS.

As in the previous example, the FVS exhibits a delay in the relaxation with respect to the SSS. It is important to note, here, that the first relaxation, although associated with a decrease of about 99% of the shear modulus $G(t)$, does not influence substantially the behavior of the laminated glass beam. In fact, the value of the shear modulus after the first relaxation, is high enough to attain the monolithic limit in the sandwich structure behavior, as recalled in Figure 5; hence, the relaxation of the structure, i.e. the increase of the maximum sag, is not noteworthy. On the contrary, it is the third relaxation, corresponding to a further decrease of the shear modulus of 90%, that strongly determines the decay in the response of the laminated glass beam. An analogous phenomenon may be observed, as it will be shown in the following Section, for commercial polymers commonly used for laminated glass.

4.3 Response of laminated glass with PVB or IP interlayers

Among the most used commercial polymeric films, PolyVinyl Butyral (PVB) and Ionoplastic Polimers (IP) are the most commonly used. Ethylene Vinyl Acetate (EVA) is also commonly
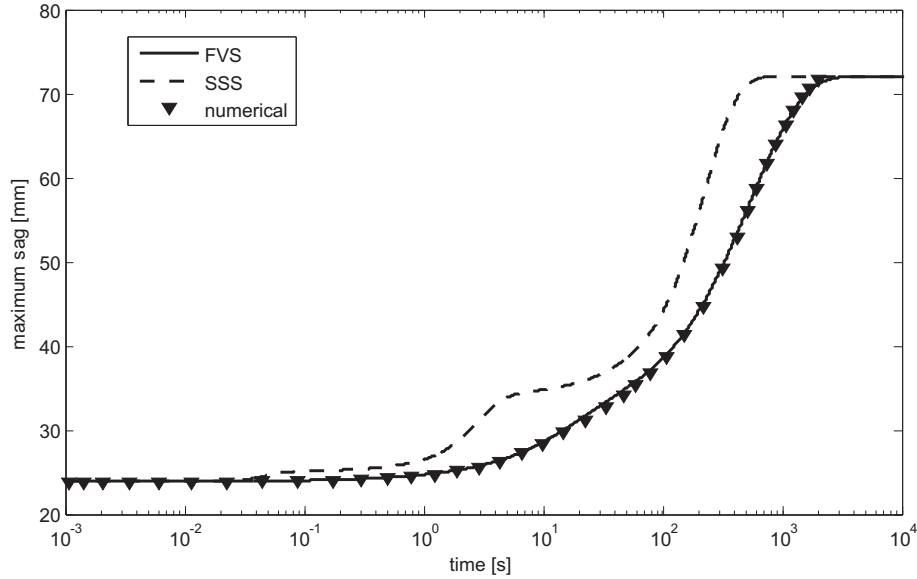
Figure 7: *Material B*: comparison of the maximum sag obtained with: the Full Viscoelastic Solution (FVS), the Secant Stiffness Solution (SSS), numerical experiments.

employed, but its viscoelastic properties are similar to those of PVB and therefore it will not be considered here.

There are many types of PVBs and IPs, and they both can be modeled by a Prony's series. Here we will consider the parameters reported in Tables 1 and 2 for PVB and IP, respectively, that have been furnished by a leader producer [7]. Such data are specific of a particular type of polymer, and may vary from material to material within the same category (PVB or IP). Therefore, the reader is strongly warned not to consider these data as universal values for design, but rather to ask for them to the producer when needed.

Figure 8 represents the comparison of the evolution in time of the maximum sag of the laminated glass beam with ionoplastic interlayer, obtained through the Full Viscoelastic Solution (FVS) and the Secant Stiffness Solution (SSS). For the considered parameters, the greatest discrepancies are approximately obtained one hour and one year after that the load has been applied. It is evident that, for times lower than, approximatively, 50 years, the shear modulus of the interlayer is high enough to attain the monolithic limit in the sandwich structure behavior (see Figure 5); hence, the relaxation of the structure, i.e. the increase of the maximum sag, is not noteworthy. However, as it is shown in Figures 9, the increasing of the sag evaluated through FVS and SSS is noticeable also for lower times. Figures 9 represent a magnification of the aforementioned graph after for times comprised between: one hour and one week; one year and 50 years. After one day, the increasing of the maximum sag predicted with the SSS may be about 13% higher than that obtained with the FVS; after one year the difference can be up to 5%. Much greater differences are

$G_0 = 471$ MPa

term index	G_i/G_0	τ_i
1	0.1606000	3.256E-11
2	0.0787770	4.949E-09
3	0.2912000	7.243E-08
4	0.0711550	9.864E-06
5	0.2688000	2.806E-03
6	0.0895860	1.644E-01
7	0.0301830	2.265E+00
8	0.0076056	3.536E+01
9	0.0009634	9.368E+03
10	0.0004059	6.414E+05
11	0.0006143	4.135E+07

Table 1: Assumed terms of the Prony's series for a particular type of PVB.

$G_0 = 375$ MPa

term index	G_i/G_0	τ_i
1	0.1271000	5.991E-12
2	0.1081000	6.240E-10
3	0.0889700	7.136E-08
4	0.0943170	2.200E-05
5	0.1150000	2.935E-03
6	0.1344000	4.620E-01
7	0.1321000	3.444E+01
8	0.0953880	8.336E+02
9	0.0570700	2.468E+04
10	0.0276820	8.071E+05
11	0.0120420	5.897E+07
12	0.0077434	9.944E+10

Table 2: Assumed terms of Prony's series for a particular type of ionoplastic polymer.

evident after 50 years of load application, as it is clear from Figure 8; however, time-scales of this order are usually higher than the usual design-life of laminated glass structures.
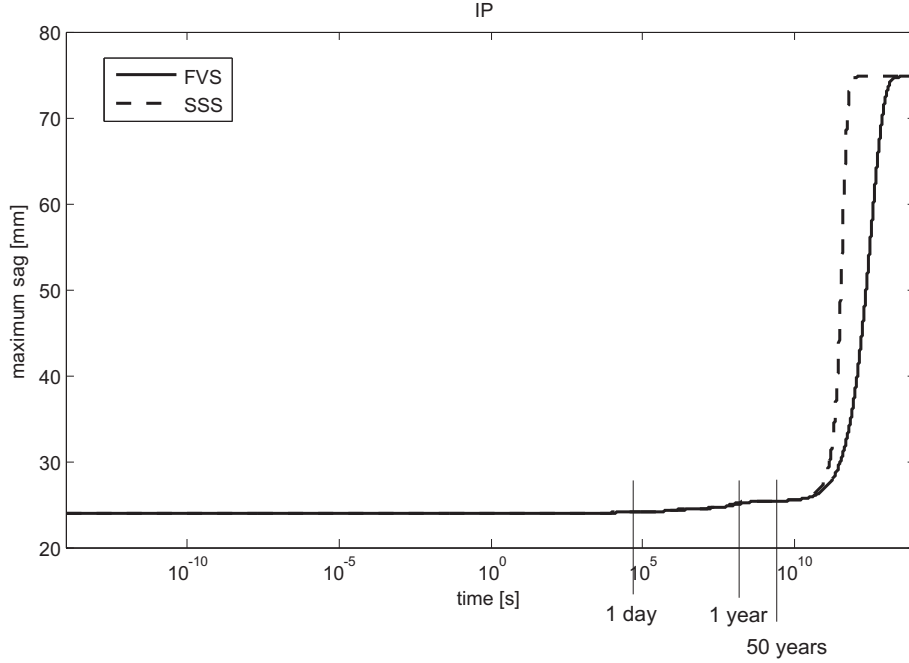

Figure 8: Ionoplastic interlayer. Comparison of evolution of maximum sag with time obtained with: the Full Viscoelastic Solution (FVS), the Secant Stiffness Solution (SSS).

Of course the times at which these differences are the most evident depends upon the parameters of the Prony's series used to model the material. Notice that, in general, such times do not coincide with the relaxation times τ_i associated with the greatest G_i, i.e., the greatest drop of the shear stiffness. In fact, one should always recall from Figure 5 that in the laminated beam the gross decay in stiffness occurs only at particular values of the shear modulus G. If the viscoelastic phenomenon does not reduces G of a sufficient amount, the laminated beam remains anchored to the monolithic limit.

Figure 10 represents the counterpart of Figure 8 for the case of PVB; from a comparison between these two pictures, one could notice that the differences between the FVS and the SSS are similar at the qualitative level. It is evident that, due to the higher decay of $G(t)$ of the PVB, the laminated glass beam attains the monolithic behavior just for times less than, approximatively, 1 s. As it is shown in Figures 11a and Figures 11b for time scale of the order of 1 day and 1 year, respectively, the difference between the maximum sag evaluated through FVS and SSS is relevant (about 5% for one year load-duration).

The greatest differences between the FVS and the SSS are again noticed at time-scales of the order of 50 years (Figure 10), but certainly within the lifetime of the structure. Differences may be up to 25%.
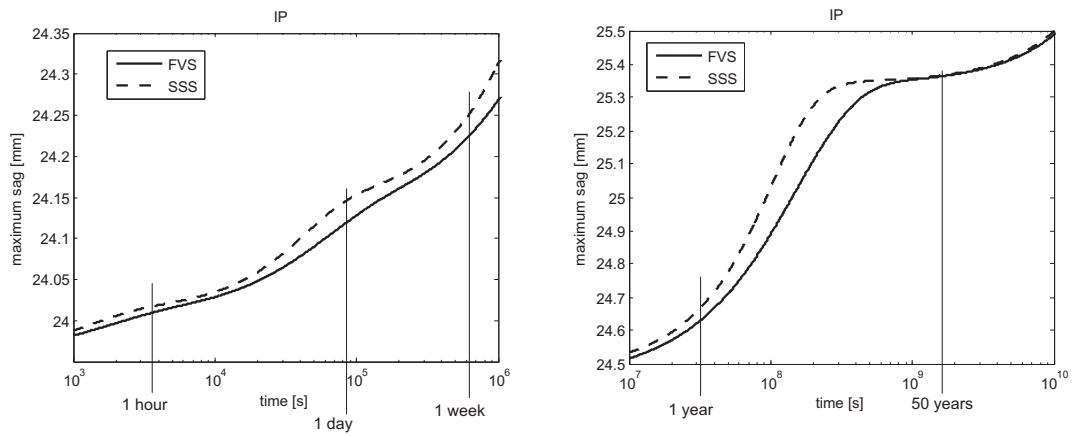
Figure 9: Ionoplastic interlayer. Magnification of the maximum sag calculated with FVS and SSS for a load duration comprised between a) one hour and one week and b) one year and 50 years.
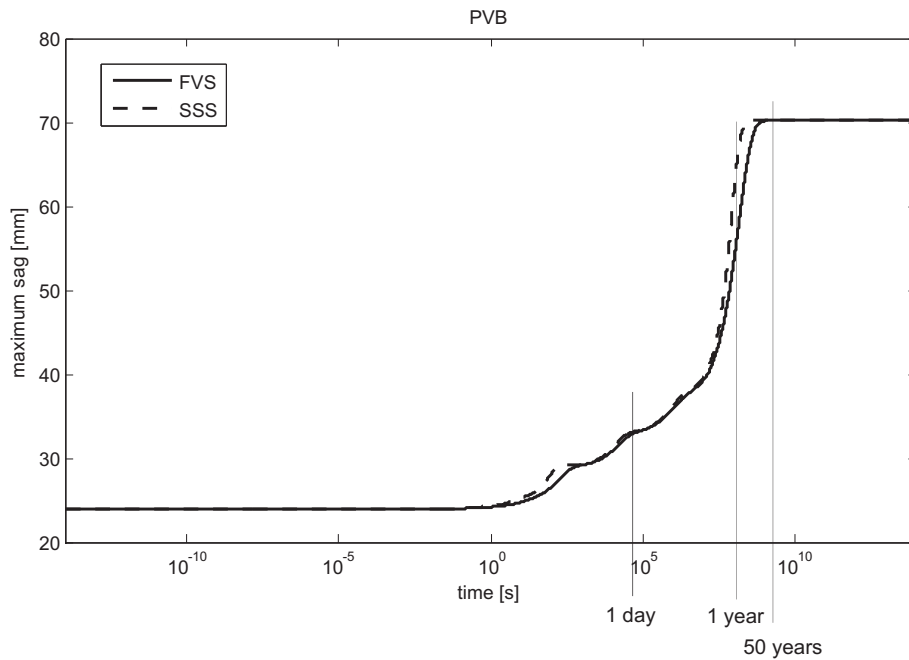

Figure 10: PVB interlayer. Comparison of evolution of maximum sag with time obtained with: the Full Viscoelastic Solution (FVS), the Secant Stiffness Solution (SSS).
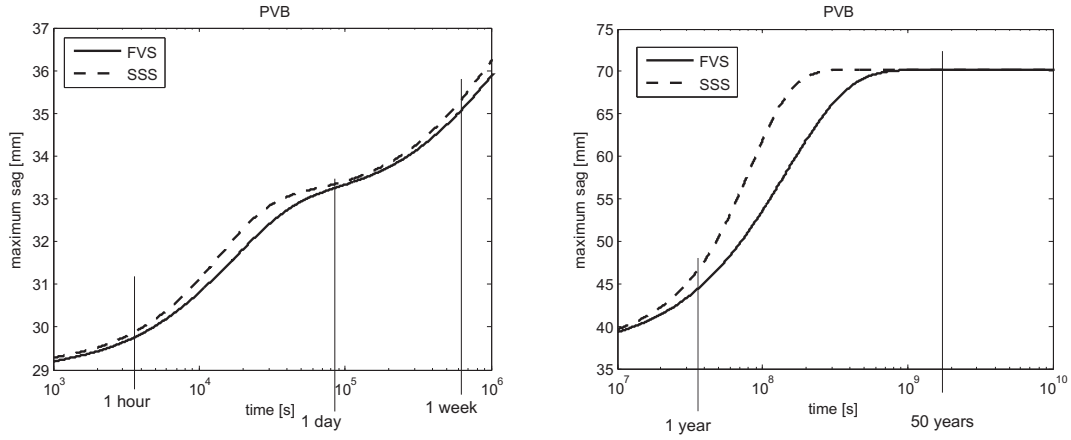
Figure 11: PVB interlayer. Magnification of the maximum sag calculated with FVS and SSS for a load duration comprised between a) one hour and one week and b) one year and 50 years.

In conclusion, IP interlayers are much stiffer than PBV interlayers, hence, they are less sensitive to viscoelastic phenomena. For PVB-laminated beams the usual practice of calculating the response through the secant stiffness approach may lead to rather conservative results.

5   Discussion and conclusions

The common practical way to calculate the response of laminated glass is to consider both glass and polymeric interlayer as linear elastic materials; the viscoelastic behavior of the polymer is considered *a priori*, by taking its equivalent elastic modulus to be the relaxed modulus under constant strain after a time equal to the whole duration of the design action. Here, we have analytically solved the time-dependent problem of a laminated-glass simply-supported beam under constant loading, modeling the viscoelastic response of the polymer by a Prony's series of Maxwell elements (Maxwell-Wiechert model).

In the case in which the shear strain imposed to the polymer is constant in time, the corresponding shear stress is decreasing in time and implies a relaxation of the material. But the value of the shear modulus so calculated according to the characteristic duration of the applied loads cannot be used in an equivalent static analysis, to evaluate stress and strain of the composite beam under constant applied loads. In fact, it takes time for the polymer to relax and, as this process progresses, also the strain of the polymeric interlayer increases in time: the corresponding stress thus depends on both the current strain and the strain history up to the current time. In particular, when the strain in the polymer is increasing with time, the relaxation of the stress is delayed with respect to the relaxation

that would result if the polymer was constantly strained at the actual value throughout its whole history. Hence, the gross response of the laminated beam is in general stiffer than it would results if calculated according to the common design practice, i.e., modeling the polymer with its relaxed modulus associated with the duration of the design action.

In general, the aforementioned delay provides a decrease of the vertical displacement of the beam itself, thus increasing the apparent stiffness of the composite structure. Hence, an increase of the shear stress, due to the effect of the viscoelastic "memory" of the polymer, leads to an increase of the overall stiffness of laminated glass.

The effect of the relaxation of the shear modulus on the overall response of the sandwich beams depends upon the order of magnitude of the shear modulus itself. A range of values of G can be defined, outside which the beams is not sensitive to the variation of the polymer stiffness. Under a threshold value, the beams behaves as a layered structure, while for high values of the shear modulus of the interlayer, the beam presents a monolithic response.

In conclusion, a full viscoelastic analysis is recommended when one is interested in a precise, non-conservative, design of a laminated glass structures. The differences between the full viscoelastic calculations and the simiplified approach that makes use of the secant stiffness of the polymeric interlayers strongly depend upon the viscoelastic properties of the material, reaching differences up to $20 \div 25\%$ for PVB interlayers, for load durations of the order of one year. Therefore, take your time in the calculations... and let the polymer relax.

References

[1] ABAQUS. *Analysis users manual, version 6.10.* Simulia.

[2] G. A. Arzoumanidis and K. M. Liechti. Linear viscoelastic property measurement and its significance for some nonlinear viscoelasticity models. *Mechanics of Time-Dependent Materials*, 7:209–250, 2003.

[3] M. Asik and S. Tezcan. A mathematical model for the behavior of laminated glass beams. *Computers & Structures*, 83(21-22):1742–1753, August 2005.

[4] R.A. Behr, J.E. Minor, and H.S. Norville. Structural behavior of architectural laminated glass. *Journal of Structural Engineering*, 119(1):202–222, 1993.

[5] S. J. Bennison and P. S. Davies. High-performance laminated glass for structurally efficient glazing. In *Innovative light-weight structures and sustainable facades*, pages 1–12.

[6] S. J. Bennison, C. A. Smith, A. Van Duser, and A. Jagota. Structural performance of laminated glass made with a "stiff" interlayer. In *Glass Performance days*, pages 1–9, 2001.

[7] S. J. Bennison and I. Stelzer. Structural Properties of Laminated Glass, short course. In *Glass performance days, Tampere (Finland)*, 2009.

[8] L. Boltzmann. Sitzungsber. *Kaiserl. Akad. Wiss. Wien, Math.-Naturwiss*, 70(2):275, 1874.

[9] B. G. Galerkin. *Rods and plates. Series in some problems of elastic equilibrium of rods and plates.* Vestn. Inzh. Tech. (USSR), 1915.

[10] L. Galuppi and G. Royer-Carfagni. Effective Thickness of Laminated Glass Beams. New expression via a variational approach. *Engineering Structures*, 38:53–67, 2012.

[11] J. A. Hooper. On the bending of architectural laminated glass. *International Journal of Mechanical Sciences*, 15(4):309–323, 1973.

[12] I. V. Ivanov. Analysis, modelling, and optimization of laminated glasses as plane beam. *International Journal of Solids and Structures*, 43(22-23):6887–6907, November 2006.

[13] J. Kim, G.A. Sholar, and S. Kim. Determination of accurate creep compliance and relaxation modulus at a single temperature for viscoelastic solids. *Journal of Materials in Civil Engineering*, 20:147–156, 2008.

[14] R. Miranda Guedes, A. Torres Marques, and A. Cardon. Analytical and experimental evaluation of nonlinear viscoelastic-viscoplastic composite laminates under creep, creep-recovery, relaxation and ramp loading. *Mechanics of Time-Dependent Materials*, 2:113–128, 1998.

[15] N. M. Newmark, C. P. Siess, and I. M. Viest. Tests and analysis of composite beams with incomplete interaction, 1951.

[16] H. S. Norville, K. W. King, and J. L. Swofford. Behavior and strength of laminated glass. *J. Eng. Mech. - ASCE*, (124):46–53, 1998.

[17] S. W. Park and R. Y.Kim. Fitting prony-series viscoelastic models with power-law presmoothing. *Journal of Materials in Civil Engineering*, 1:26–32, 2001.

[18] A. D. Polyanin and A. V. Manzhirov. *Handbook of Integral Equations.* Chapman & Hall/CRC Press, 1998.

[19] E. Wiechert. Gesetze der elastischen nachwirkung fr constante temperatur. *Annalen der Physik*, 286(11):546–570, 1893.

[20] M. L. Williams, R. F. Landel, and J. D. Ferry. The temperature dependence of relaxation mechanisms in amorphous polymers and other glass-forming liquids. *Journal of the American Chemical Society*, 77(14):3701–3707, 1955.